

Extinction Characteristics of Six Tremolites with Differing Morphologies

Matthew S. Sanchez, Richard J. Lee, and Drew Van Orden
RJLee Group Inc.*

KEYWORDS

Tremolite, amphibole, fibrous, morphology, extinction angle.

ABSTRACT

There has been considerable discussion in the literature related to the use of standard optical properties of commercial asbestos minerals for the classification of amphibole minerals found in raw materials as either asbestiform or as non-asbestos (1-4). The goal of this study was to ascertain if there is a relationship between particle morphology and extinction characteristics in monoclinic tremolite amphiboles. Six tremolitic amphiboles were chosen for this study: three are fibrous (five from natural sites (i.e., mining locales)) and one is the NIST SRM 1867a tremolite standard. The morphology of these tremolites ranged from blocky to asbestiform. A particle-by-particle analysis was performed to determine extinction characteristics and the number of EPA-defined asbestos characteristics. In general, zero or near-zero extinction angles correlate to the number of asbestiform characteristics. Exceptions to this occur when a non-fibrous tremolite has (100) parting as a result of twinning or when fibrous tremolites are elongated in the *a*-crystallographic direction, therefore preferentially lying on (010). However, when using extinction characteristics in conjunction with morphology, the differences between habit is discernable. The three fibrous tremolites have different fiber widths and, as such, exhibit different extinction characteristics. The smaller the diameter of the fibers, the greater number of particles exhibiting parallel extinction. The sample with the smallest widths (< 0.5 μm) displayed parallel extinction for all

particles. When fiber diameters are small (<1 μm) optically visible fibers are in fact bundles of fibrils and are not single crystals; they therefore show parallel extinction.

INTRODUCTION

The asbestiform habit is a unique mineral growth characteristic in which minerals form as bundles of randomly oriented ultra-fine fibrils weakly bound together. The individual fibril surfaces develop during crystallization and are not a result of fracture, cleavage or parting. The fibrillar structure of optically biaxial asbestiform minerals (i.e., the amphiboles) results in uniaxial-like properties, when examined using polarizing light microscopy (PLM) (1). As a result, asbestiform bundles of monoclinic amphiboles of sufficient dimension to be visible in the PLM, have parallel or near parallel extinction. In addition to defining the optical properties of asbestiform bundles, the unique growth mechanism of the asbestiform habit is fundamentally responsible for the widely recognized properties of asbestos: namely flexibility and tensile strength. These same characteristics are also generally accepted as the underlying reason for the adverse health effects of commercial amphibole asbestos fibers (2,3). The long, thin, readily separable fibrils can penetrate and lodge in the air exchange portion of the lung where they ultimately provoke disease. In natural ore or rock, asbestos fibers form in parallel or radiating bundles generally occurring in veins. They generally have a smooth silky fibrous appearance and can be teased into matted balls or bundles when lightly abraded.

*350 Hochberg Rd. Monroeville PA, 15146

Microscopically, the asbestiform crystal habit is defined by the following specific morphological characteristics (4):

1. Mean aspect ratio for individual fibers (not bundles) ranging from 20:1 to 100:1 or higher for fibers longer than five micrometers.
2. Very thin fibrils, usually less than 0.5 micrometers in width.
3. Two or more of the following:
 - a. Parallel fibers occurring in bundles
 - b. Fiber bundles displaying splayed ends
 - c. Matted masses of individual fibers
 - d. Fibers displaying curvature

The published PLM analytical methods, written for the analysis of commercial products that may contain asbestos, vary somewhat in optical characteristics for asbestiform particles. Most describe the extinction angle of the monoclinic asbestos minerals as being at or near zero degrees (5-7). The NIOSH 9002 method (8) differs slightly from most other methods in that it specifically describes tremolite-actinolite asbestos as having oblique extinction in the range of 10-20°. Tremolite and actinolite have extinction angles in this range, although in regard to asbestiform tremolite and actinolite, the source of this statement is unknown. A more recent study by Verkouteren and Wylie (9) described fibrous tremolite-actinolite that contains some fibers with diameters greater than one micrometer in diameter, exhibiting oblique extinction, with normal biaxial optical properties. They do not include any fibril width data and state that these amphibole fibers do not adhere to the definition of asbestos (i.e., fiber widths < 0.5 µm).

Asbestos identification in building products such as pipe insulation, fireproofing, and plaster has become a routine laboratory service in more than 150 laboratories around the nation. Laboratories are certified to conduct these analyses by the American Industrial Hygiene Association (AIHA), National Voluntary Laboratory Accreditation Program (NVLAP), and/or state accreditation bodies based on the proficiency of their analysts, together with other criteria. Commercial products offer nearly ideal material for routine laboratory asbestos analysis, because of their use in commercially produced asbestos.

In commercial products, non-asbestiform amphiboles represent an insignificant source of interference due to the mining and milling process that is designed to separate the valuable asbestos fiber from the host rock. Therefore, PLM methods (4,8,10) and the Code of Federal Regulations (11) were written with the pre-

sumption that the mineral fibers in the building product were commercially produced. These procedures are readily and easily applied to building products by well-trained analysts. The goal of most analyses is simple: Is there asbestos present in quantities greater than one percent? Little or no attention is paid, in routine analysis, to any non-asbestos fragments of serpentine or amphibole. The analytical challenge primarily involves estimation of the abundance of the asbestiform species in different matrices.

Environments that potentially contain non-commercial asbestos are of significance today (12), ranging from locations such as New Caledonia (13) to California (14) to Italy (15). In these environments, asbestiform minerals are present naturally; the assumption that non-asbestiform amphiboles represent an insignificant interference is generally invalid. Unlike bulk manufactured products, mixed mineral samples are not homogeneous because they have not been processed or refined for commercial purposes. Any asbestiform minerals, including any non-asbestiform amphibole in the same formation, remain mixed with other minerals common to ultramafic rock and dolomitic marble formations.

The principal analytical challenge is to distinguish asbestiform particles from elongated cleavage fragments. The term cleavage is defined as the fracturing of a mineral along systematic planes of weakness determined by the atomic lattice structure of the mineral. Orthorhombic amphiboles have a (210) cleavage plane; monoclinic amphiboles have a (110) cleavage plane; these are really the same plane but the "2" for orthorhombic amphiboles refers to a doubling of the spacing along the *a* crystallographic axis with monoclinic crystals. A cleavage fragment is a particle that has been broken from another larger particle. Elongated amphibole cleavage fragments are produced from massive acicular or prismatic crystals during weathering or from a mechanical fracture. Cleavage fragments and unfractured single crystals have been collectively referred to as cleavage fragments. Cleavage fragments do not tease into bundles and are not flexible, smooth or silky. As a general rule by PLM, cleavage fragments are defined by Wylie (16) as:

1. Exhibit mean aspect ratios less than 20:1 except in the case of byssolitic fibers.
2. Have parallel or stepped sides.
3. Have blunt ends or tapered ends, with characteristic terminations approximating (001) or (011) crystal planes.

4. Habits ranging from blocky to prismatic to columnar to acicular.

5. Do not occur in bundles, do not exhibit splayed ends, significant curvature or flexibility.

Morphological distinctions between fibers and cleavage fragments have historically been supplemented by evaluation of the extinction angle of particles. The extinction angle in this sense is not the true angle $c^{\wedge}Z$, but $c^{\wedge}Z'$ and is the angle between the long axis of the mineral and the vibration direction in the plane of the microscope stage nearest to parallel with the long axis. Recently, questions have arisen as to the validity of the extinction angle as a discriminator between asbestiform and non-asbestiform particles in the natural environment (17,18). Therefore, a study to evaluate the relationship between extinction angle and the morphological characteristics on a particle-by-particle basis from non-commercial asbestos sources was undertaken here.

SAMPLE PREPARATION AND MEASUREMENTS

Six tremolite samples were chosen for this study ranging in morphology from massive to fibrous. Five of the samples come from mixed mineral environments (mines or quarries); the sixth sample is the NIST SRM 1867a tremolite. The first two samples; Arnold_1 and Arnold_2, come from the Arnold talc mine in New York State. The other three samples from mixed mineral environments come from Ala di Stura, Italy;

Jamestown, California; and North Carolina. The first two of these samples were used in an injection study by Davis that showed the Jamestown tremolite as more hazardous than the Ala di Stura (19). The current paper is in no way an evaluation of the carcinogenicity of the tremolite samples relative to each other or in general; however, since health study data does exist on these samples, it is appropriate to reference it. The NIST tremolite originates from the Conda deposit near Barstow, California, and was used in a study by Brown (20). The North Carolina tremolite was collected just west of Raleigh, North Carolina in a greenschist facies ophiolite. Descriptions of the samples are given in Table 1, and photographs are shown in Figure 1.

Each sample was lightly ground using a mortar and pestle and then sieved to $-150\ \mu\text{m}$ and $+125\ \mu\text{m}$. Grain mounts were then prepared in refractive index liquid $n = 1.550$. Exceptions were the Jamestown and North Carolina tremolite for which, due to their fibrous habit, crushing was ineffective and only matted the mineral. For these samples, the mineral was cut first with a razor blade to around $0.5\ \mu\text{m}$ in length, suspended in acetone, and ultra-sonicated to separate the fibers. The particles were then placed on a glass slide and the acetone evaporated.

Systematic measurements were made starting at one corner of the slide. Each slide was then moved horizontally and each particle in the field of view was measured to reduce any systematic error by the analysts and to avoid biasing the measurements towards certain morphologies. A total of 150 measurements

TABLE 1: MACRO DESCRIPTIONS AND ORIGINS OF SAMPLES

Name	Picture	Dominant Mineral	Description	Location
Arnold_1	Figure 1a	Tremolite	Massive	Arnold Mine NY
Arnold_2	Figure 1b	Tremolite	Massive to Acicular	Arnold Mine NY
Ala d'Stura	Figure 1c	Tremolite	Acicular	Ala d'Stura Italy
NIST 1867a	Figure 1d	Tremolite	Fibrous	Conda Deposit, Barstow CA
Jamestown	Figure 1e	Tremolite	Fibrous	Near Jamestown CA
North Carolina	Figure 1f	Tremolite	Fibrous	Near Raleigh NC

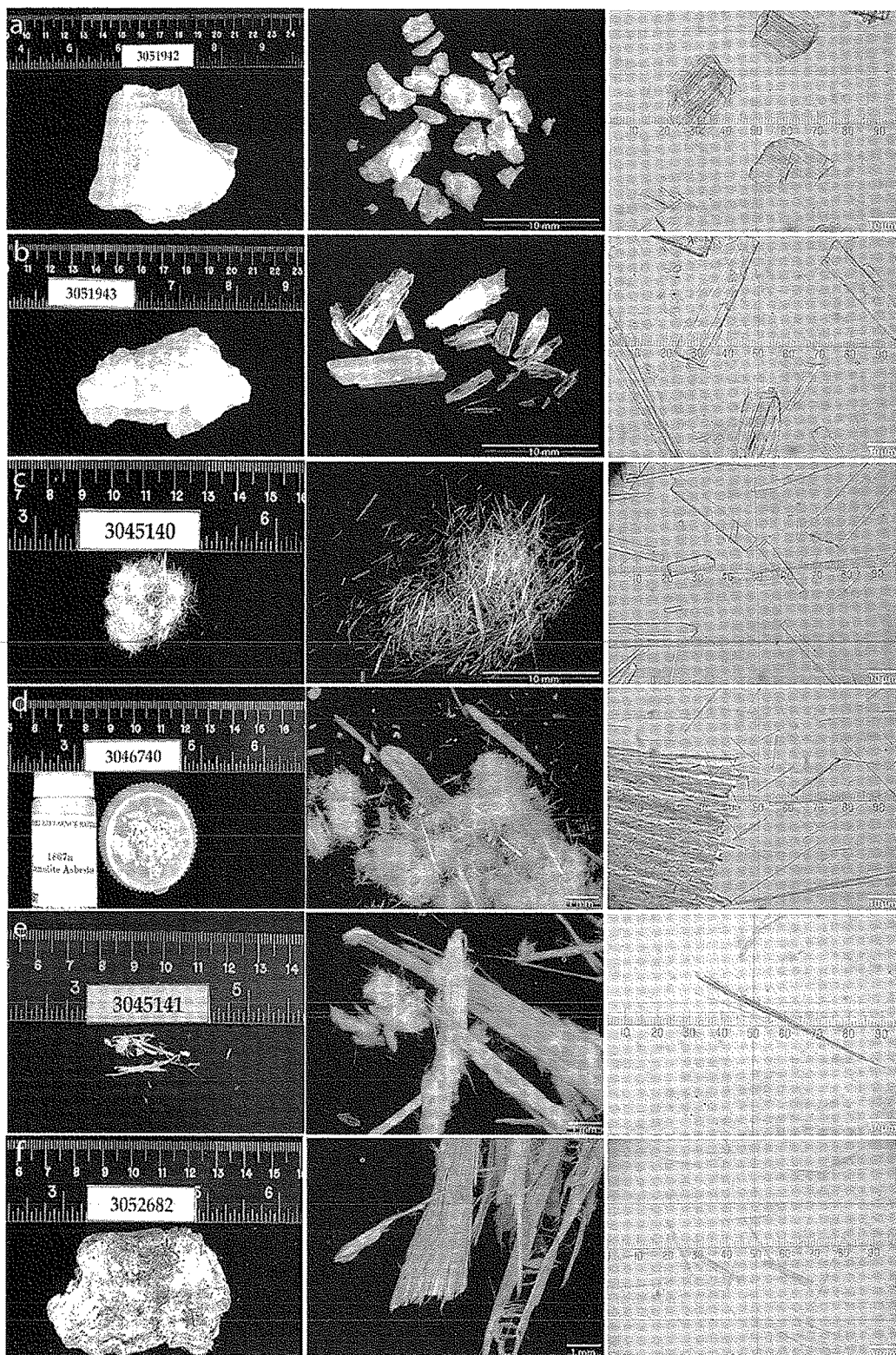


Figure 1: Hand sample, macro- and micro- photographs of each of the six tremolite samples used in this study: (a) Arnold_1, (b) Arnold_2, (c) Ala di Stura, (d) NIST SRM 1867a, (e) Jamestown, and (f) North Carolina.

were taken. Each particle's length, width, and extinction angle was measured and determinations of the number of asbestiform characteristics were then made. The criteria for asbestiform characteristics are based on the EPA Method for the "Determination of Asbestos in Bulk Building Materials" (4) as described previously.

Extinction characteristics on (100) and (010) cleavage fragments and true extinction angle measurements were obtained using spindle-stage assisted PLM. Individual particles were mounted on a glass fiber with their c -crystallographic directions parallel to the spindle rotation axis (9). The particle was then brought parallel to the polarizer and rotated about the spindle axis until it was extinct. This position is (100). The particle was then rotated in 10° increments about the spindle axis and the extinction angle was measured. At 90° from (100) is (010) and the true extinction angle. 2V values were calculated using the methods described by Bloss (21) and the computer program EXCALIBUR.

Scanning electron microscopy (SEM) images were obtained using a FEI Sirion 400 FESEM operated in the "ultrahigh resolution" mode with a Through-The-Lens Detector (TLD) and an accelerating voltage of 3 kV, a beam current of 200 pA, and a 4.0 mm working distance. Bundles were glued to a glass slide and in the case of the Jamestown tremolite were glued to a glass fiber on a goniometer pin, following Bandli (22).

SAMPLE DESCRIPTIONS

Figure 1 is a series of photographs for each of the samples showing (from left to right): the bulk sample, a stereomicroscope image, and PLM in plane polarized light. The samples are described below. The progression from blocky to elongate to fibrous habits is evident in the figure. A description of each sample is given below.

Arnold 1: Figure 1a

In plane polarized light, the particles are colorless with predominantly blocky morphology, though columnar and acicular particles are also present. Particle ends are orthogonal, stepped and uneven. A majority of particles clearly show the (110) cleavage trace.

In crossed polars, the maximum and minimum interference color seen is 2nd order blue and 1st order grey. Particles with the cleavage trace visible, consistently exhibit lower retardation, typically 1st order yellow. Particles show positive elongation and therefore are length slow. Optical class is biaxial (-), 2V was

calculated at 71.9° ($\pm 2.1^\circ$). The extinction angle was measured at 15.4° .

Arnold 2: Figure 1b

In plane polarized light particles are colorless with predominantly blocky morphology. However, they are more elongate than the Arnold_1 sample. There are also columnar and acicular particles present. Cleavage traces can be seen but are not as prevalent as the Arnold_1 tremolite. Particle ends are orthogonal, uneven, and stepped.

In crossed polars, the maximum and minimum interference color seen is 2nd order green and 1st order grey. A small number of particles exhibit undulatory or incomplete extinction. Particles are length slow and are biaxial (-) with 2V calculated at 79.7° ($\pm 1.0^\circ$). Extinction angle was measured as 14.7° ($\pm 2.0^\circ$).

Ala di Stura: Figure 1c

In plane polarized light, the absorption color is pale green to yellow with no pleochroism. Crystal morphology is elongated and ranges from bladed to acicular to uneven. Particle ends, regardless of overall morphology, are either orthogonal or stepped. Two planes of cleavage are discernible.

In crossed polars, the maximum and minimum interference color seen is 2nd order blue and 1st order grey. Particles are length slow. Optical class is biaxial (-).

The Ala di Stura was one of the samples evaluated by Verkouteren (23), with measured refractive indices, 2V, extinction angle, and composition: $\alpha = 1.612$, $\beta = 1.6278$, $\gamma = 1.638$, $2V = 78.2^\circ$, and $c^\wedge Z = 17.2^\circ$. Ferroactinolite content is reported as $X_{Fe} = 9.1\%$.

NIST SRM 1867a: Figure 1d

In plane polarized light, two distinct morphologies are present; bundles and fibers. The fibers originate from the bundles, but because of their widths (i.e., $> 0.5 \mu m$), these fibers would have historically been classified as byssolite. Also, they appear to be single crystals and not small fiber bundles. The bundles and fibers are colorless and the single crystals show two planes of cleavage. The morphology of the single crystals ranges from the majority being bladed or acicular with a few particles being blocky. The bundles are straight and ends are splayed. Ends of the fibers are orthogonal, stepped, and uneven.

In crossed polars, the maximum and minimum retardation for the bundles are 2nd order blue to 1st order grey, while the single crystals exhibit 1st order

yellow to 1st order grey. Optical properties of this tremolite are certified and reported by NIST (24).

Jamestown CA: Figure 1e

In plane polarized light, colorless bundles and fibers are visible. The majority of fibers appear to be single crystals, although in this sample some are clearly smaller bundles, similar to the NIST sample. The fibers were not classified as asbestos due to their widths. The fibrosity of this sample is finer than that of the NIST. Fiber morphologies are acicular with ends either orthogonal or uneven.

In crossed polars, the maximum and minimum interference color observed in the bundles is 1st order red and 1st order grey. The single crystals exhibit near maximum retardation of 1st order grey and minimum of near zero retardation. Bundles and particles are length slow. Optical class is biaxial (-).

The Jamestown tremolite was one of the minerals evaluated by Verkooren (23), with measured refractive indices, 2V, extinction angle, and composition: $\alpha = 1.606$, $\beta = 1.623$, $\gamma = 1.632$, $2V = 71.4^\circ$, and $c^\wedge Z = 16^\circ$. Ferro-actinolite content is reported as $X_{Fe} = 7.9\%$.

North Carolina: Figure 1f

In plane polarized light, this sample is colorless. The fiber size is very fine, on the order of 0.3 μm . Fibers derived from the bundles appear to be smaller fiber bundles as opposed to single crystals. Fiber bundles show splays, significant curvature, and high aspect ratio.

In crossed polars, the maximum and minimum interference color observed is upper 1st order grey and lower 1st order grey. The bundles are all length slow and the optical class is biaxial (-). Refractive indices in grain mount are consistent with tremolite. Powder X-ray diffraction also confirmed that tremolite is present.

RESULTS AND DISCUSSION

The number of particles that were above and below an extinction angle of 8° (as well as the number of asbestos characteristics) is shown for the mineral samples in Table 2. The value of 8° was chosen as a "cut-off point" due to the relationship between apparent extinction and crystal orientation. A tremolite with (100) parting and therefore lying on the (100) face, or a mass of randomly oriented fibers, will have an apparent extinction angle $< 8^\circ$. Conversely tremolite cleavage fragments have a tendency to rest on the (110) face and will exhibit extinction angles $> 8^\circ$ (see Figure 4 for a graphical representation). In general, the extinction angle decreases as the number of asbestos characteristics increase. The exception to this is the Arnold_1 tremolite from the Arnold talc mine in New York.

The Arnold_1 tremolite exhibits a near zero extinction angle due to (100) twinning; this sample does not possess a fibrous morphology. Figure 2 illustrates optical techniques used to measure the extinction angle and determine the crystallographic direction in a mineral. Figure 2a shows a particle in plane polarized light, the (110) cleavage trace is visible as the lineations running east-west. These lineations are cleavage traces and not fibers. Figure 2b shows the same crystal in crossed polars with the full wave plate inserted. The angle between the c-crystallographic axis and the polarizer is 0° . Figure 2c is the same grain viewed conoscopically showing two isogyres and a near-centered acute bisectrix. In the case of the tremolite-actinolite series, the acute bisectrix is seen when the crystal is oriented such that (100) is in the plane of the microscope stage (i.e., when you are looking down the a-crystallographic direction).

Figure 3 is a grain from the Arnold_1 sample showing inclined extinction. Figures 3a and 3b are the same grain shown in plane and crossed polarized light. Also,

TABLE 2: EXTINCTION ANGLES PLOTTED WITH # OF ASBESTOS CHARACTERISTICS MET

# of Criteria Met	Arnold_1		Arnold_2		Ala d'Stura		NIST 1867a		Jamestown		North Carolina	
	0-8°	>8°	0-8°	>8°	0-8°	>8°	0-8°	>8°	0-8°	>8°	0-8°	>8°
	0	0	0	0	0	0	1	0	38	19	149	0
	2	0	0	0	5	6	25	17	28	29	1	0
	118	30	17	133	82	57	76	31	13	23	0	0

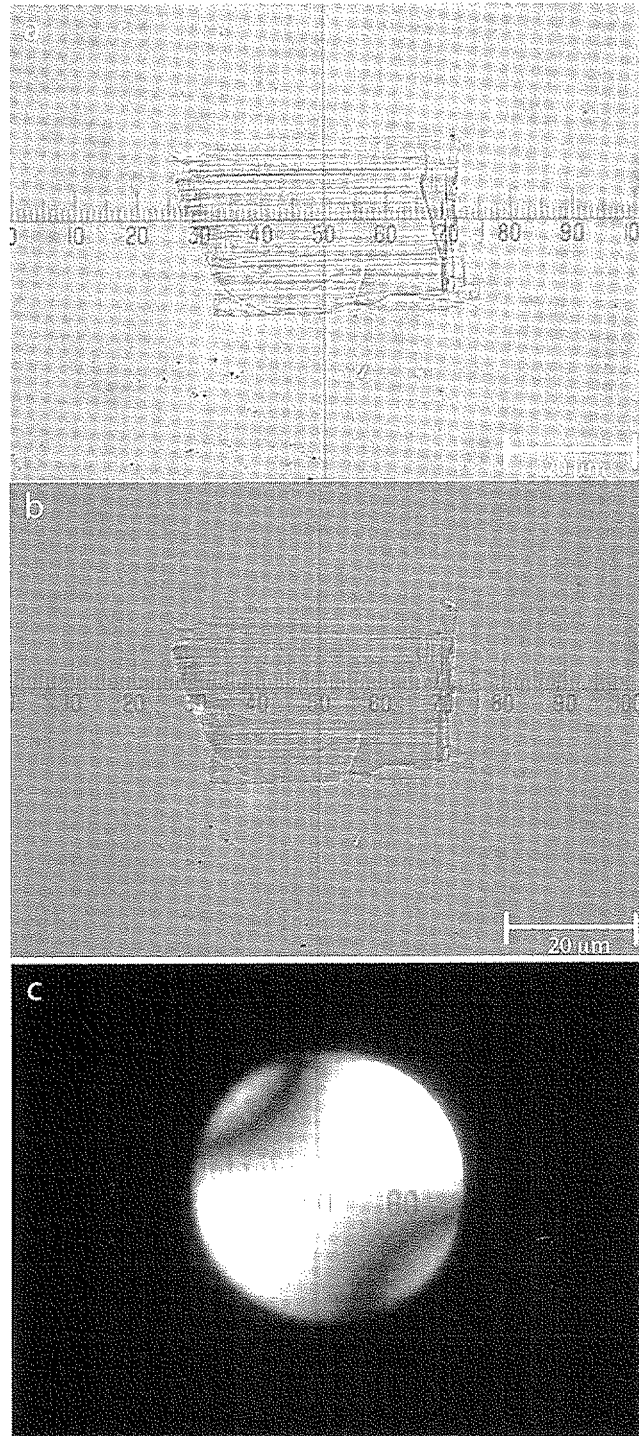


Figure 2: Photomicrographs of a grain from the Arnold_1 sample displaying parallel extinction: (a) The grain in plane polarized light with (110) cleavage traces. (b) Grain in cross polars with the full wave plate inserted. This grain exhibits parallel extinction. (c) Interference figure of this grain. Both isogyres are visible; this figure is a near-centered acute bisectrix.

notice the lack of the same lineation (cleavage trace) as seen in the previous example. This grain is lying on the (110) cleavage surface. Figure 3b is the grain rotated to extinction; the angle measured is 12.1° . This grain rotated 45° from extinction shows higher order retardation on the upper end, therefore the cross section of this grain is inferred as a wedge. Figure 3c is the interference figure for this particle; it is no longer a centered acute bisectrix. The acute bisectrix seen in Figure 2d is rotated approximately 30° from the center and one optic axis is just outside the field of view. The extinction angle, retardation, and interference figure are consistent with a monoclinic amphibole lying on or near the (110) cleavage plane.

Figure 4 is a plot of the measured extinction angle with respect to grain orientation parallel to the c -axis. At (010), defined as 0° , the true extinction angle is seen. Rotation of a grain to 60° gives the extinction angle measured directly on (110) while another 30° rotation brings the (100) plane parallel to the microscope stage, resulting in an extinction angle of 0° . This is modified from Su (25) and calculated as a function of orientation to a known $2V$ and extinction angle. Plotted are the Arnold_1 and Arnold_2 tremolite data. The orientation of grains is inferred by the measured extinction angle. The cluster of points of the Arnold_1 sample shows that the majority of grains are near or on (100), while the majority of grains from the Arnold_2 sample are on or near the (110). Interestingly, the mean and median extinction values for the Arnold_2 tremolite are 13.5° , and this value, according to the model, puts the mean measured extinction angle within one degree of (110).

Conoscopic examinations of interference figures obtained from bundles of the NIST, Jamestown, and North Carolina samples showing parallel extinction also surprisingly show what appear to be centered or near centered acute bisectrix interference figures. The isogyres become more diffuse in the North Carolina sample. Whether these bundles are all lying on (100) or if this is some optical effect created by multiple randomly oriented fibers is unclear. In both the NIST and Jamestown tremolites, a majority of the bundles exhibit parallel extinction, while a majority of apparent single crystals (fibers) from the bundles that could be measured show inclined extinction. In the Jamestown tremolite, 18 particles classified as bundles did show extinction angles greater than 8° . Mounting bundles on pins and placing them in the FE-SEM revealed the cause. Figure 5 is a series of images of the Jamestown tremolite. Figure 5a shows the end of a small bundle of fibers. There is an equiaxial fiber indicated along with

two other wider (approximately $1\ \mu\text{m}$) fibers. Figure 5b and 5c show fibers elongated in the b -crystallographic direction with the (110) and (010) faces marked. The majority of fibers observed using the SEM have this overall shape. Therefore, bundles of fibers from the Jamestown specimen are commonly aligned single crystals lying on or near the (010) plane and therefore exhibit extinction characteristics consistent with non-fibrous monoclinic amphiboles.

The North Carolina sample does not contain single crystals at PLM resolution, only smaller bundles, and these bundles display parallel extinction. Extinction angles of the NIST and Jamestown single crystals are consistent with grains lying on the (110) cleavage face (i.e., $>8^\circ$). These same properties have been described by Wylie (9) for amphibole fibers of the tremolite-actinolite-ferroactinolite series.

Table 3 lists measured grains grouped by aspect ratio for each sample. Each grain was defined as a bundle, fragment, or fiber. The fiber category was based on the width of the particle as $<0.5\ \mu\text{m}$. The distribution of aspect ratios show a transition from massive to more elongate to fibrous amphiboles.

The Jamestown and NIST tremolites show some interesting differences. If the width of the Jamestown fragments classified as fibers were raised from $0.5\ \mu\text{m}$ to $2.5\ \mu\text{m}$, then 27% would be fibers with 85% of those having aspect ratios greater than 20:1. This raises an important issue. It is common to assume, with a fibrous amphibole, that the fibers coming from a bundle are not single crystals but simply another fiber bundle. In the case of the Jamestown tremolite, this assumption could be correct and for the North Carolina this assumption is correct. However, in the NIST tremolite, if we again raised the width used to define a fiber from $0.5\ \mu\text{m}$ to $2.5\ \mu\text{m}$, then only 5.3% of fragments would be classified as fibers with 12.5% of those having aspect ratios greater than 20:1. In general, the fibers of the NIST are bigger than those of the Jamestown. Another study involving the NIST (20) concluded that many fibers appearing to be single crystals from the NIST tremolite (upon rotation parallel to the c -axis, using a spindle stage) appear in fact to be bundles and the NIST tremolite (based solely on morphologic criteria) contains only 19% asbestiform fibers. Thus, all fibrous amphiboles are not created equal and not all fibrous amphiboles have the unique morphological, physical, and chemical characteristics of asbestos.

Each particle measured in the North Carolina tremolite was classified as a bundle. In the case of the North Carolina tremolite, individual fibrils are below the resolving power of the PLM. In non-commercial

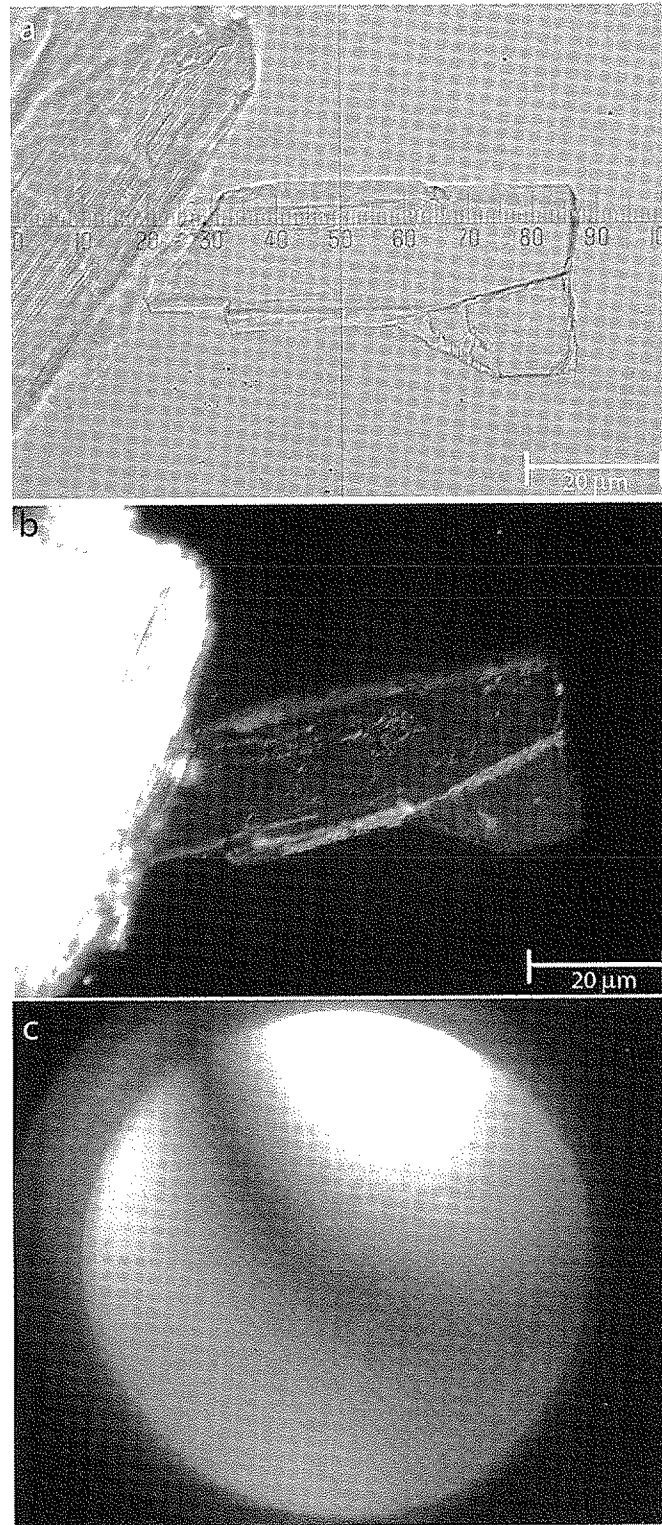


Figure 3: Photomicrographs of a grain from the Arnold_1 sample displaying inclined extinction: (a) Grain in plane polarized light with the c-axis parallel to the lower polarizer. Notice the lack of the cleavage trace. (b) Grain rotated to extinction; the angle between the c-axis and the lower polarizer is around 12° . (c) Interference figure of this grain. Only one isogyre is visible and one optic axis is just out of the field of view in the lower left quadrant.

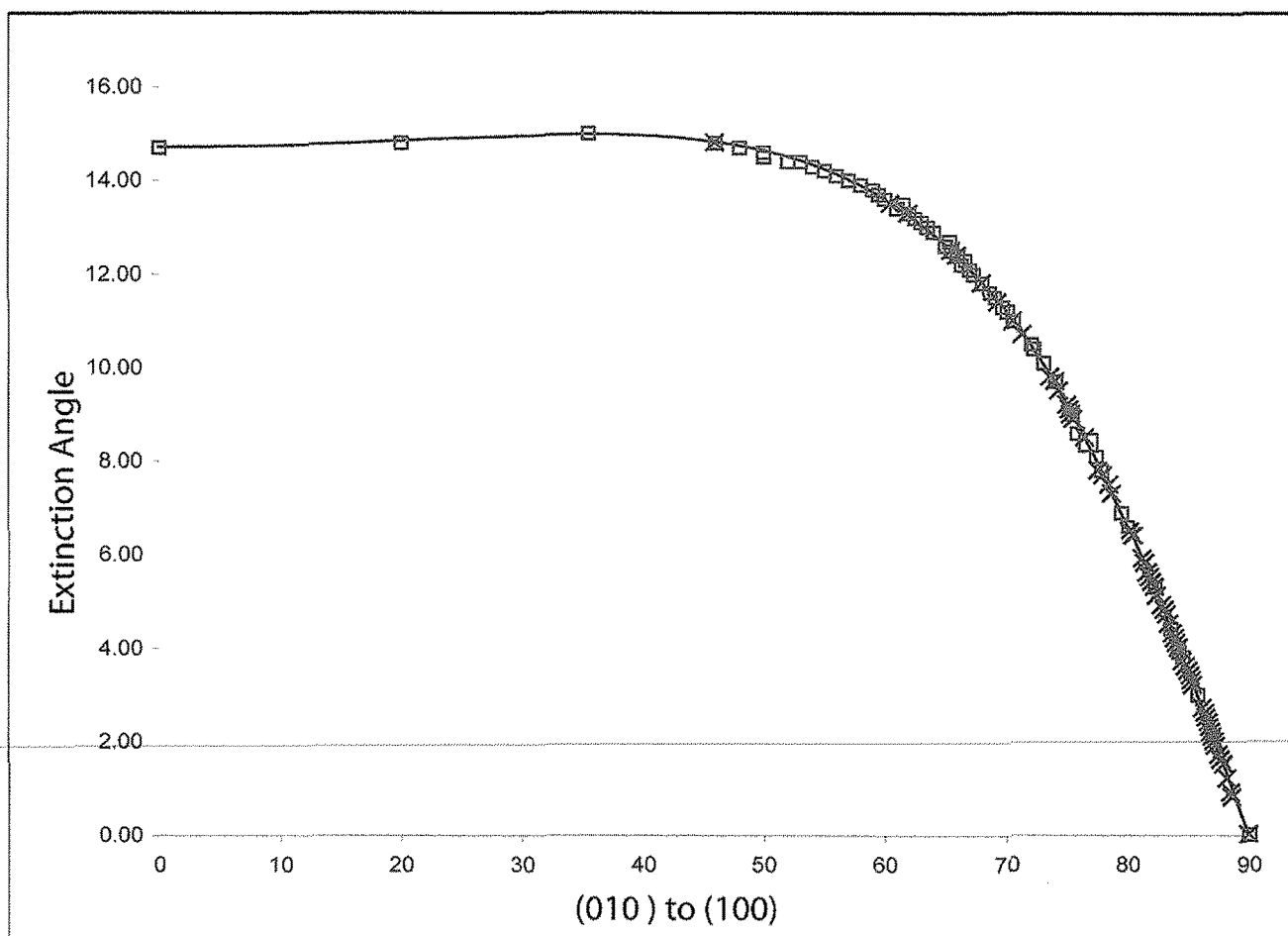


Figure 4: Graph illustrating the measured extinction angles of the Arnold_1 marked as an x and the Arnold_2 marked with an open box. The dashed line is the model. The respective clusters are near (110) for the Arnold_2 and (100) for the Arnold_1.

settings, the fiber diameters need to be addressed, in order to accurately characterize and discriminate between asbestiform and non-asbestiform amphiboles.

Figure 6 shows SEM images of bundles from the: a) NIST, b) Jamestown, and c) North Carolina tremolites. Measurement of fiber length, width, and diameter for the three fibrous samples, by either SEM or TEM is beyond the scope of this study; however, it is evident from the photomicrographs that the degree of fibrosity varies from sample to sample.

CONCLUSIONS

The increase in the number of asbestos characteristics and near zero extinction angles is directly related to the fibrillar growth habit. The level of fibrosity

(i.e., how fine the fibril widths are) can be inferred by the extinction characteristics of a population of fibers by PLM and so the asbestiform nature of the sample may be evaluated. Large fibers, resolvable and measurable by light microscopy, will tend to exhibit oblique extinction if they are single crystals. Regardless of size, fiber bundles with asbestiform fiber widths will tend to exhibit parallel extinction. The exceptions are when a non-fibrous amphibole is also twinned on (100) as seen in the Arnold_1 sample, though these particles rarely exhibit any of the accepted asbestiform morphology characteristics. This means that the other morphological characteristics of asbestos must be taken into account when evaluating amphiboles. The other exception is when a fibrous amphibole has both a fibrosity of sufficient dimensions (i.e., resolvable by

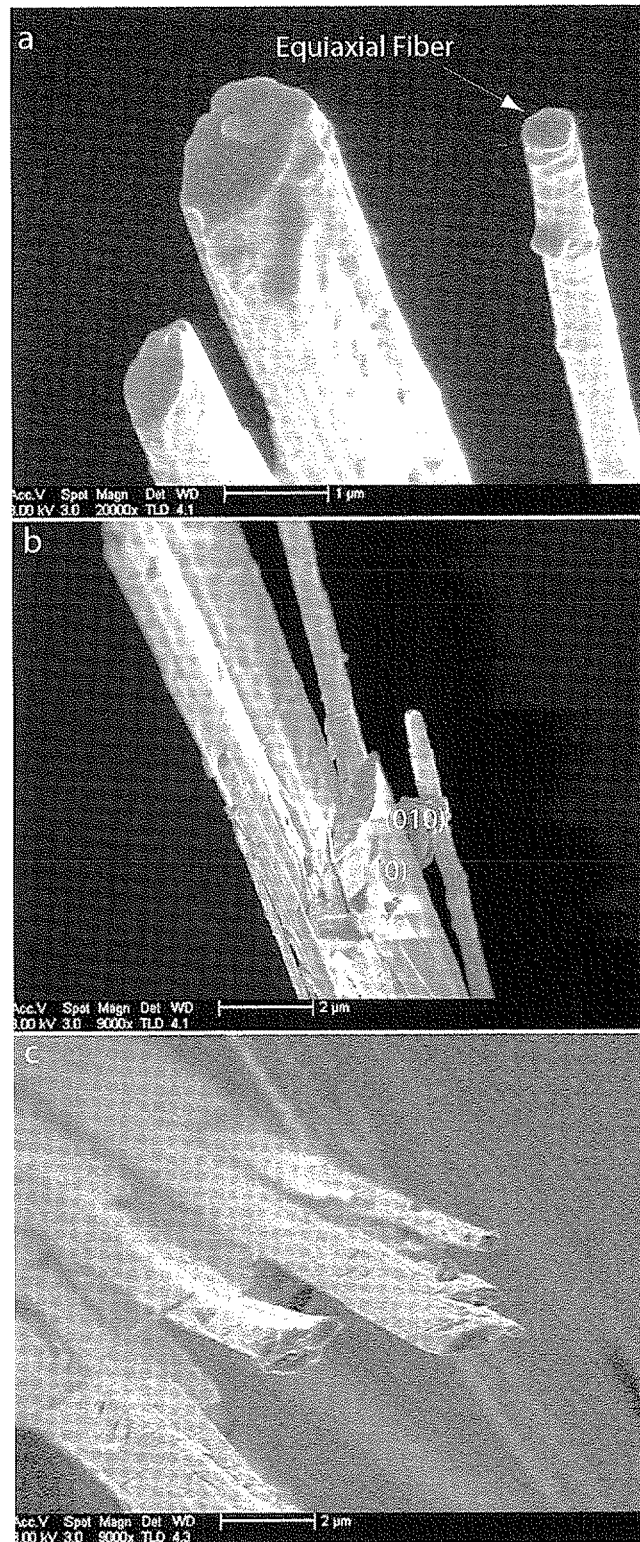


Figure 5: SEM images of bundles from the Jamestown tremolite mounted to the end of a glass fiber. (a) Bundle end containing a equiaxial amphibole fiber. (b) Bundle showing a fiber with distinct (110) and (010) crystal faces. (c) Fiber bundle end again showing the (110) and (010) faces.

TABLE 3: ASPECT RATIO GROUPING BY PARTICLE CLASSIFICATION. FIBERS WERE STRICTLY BASED ON WIDTHS <0.5 MM.

Sample	Aspect ratio	Bundles	Fragment	Fibers
Arnold_1	<3	1	107	0
	3-5	2	33	0
	6-10	0	4	0
	11-20	0	1	0
	21-50	0	0	1
	51-100	0	1	0
	>100	0	0	0
Arnold_2	<3	0	77	0
	3-5	0	44	0
	6-10	0	25	0
	11-20	0	4	0
	21-50	0	0	0
	51-100	0	0	0
	>100	0	0	0
Ala d'Stura	<3	0	17	0
	3-5	0	37	0
	6-10	0	58	0
	11-20	0	29	0
	21-50	0	8	1
	51-100	0	0	0
	>100	0	0	0
NIST	<3	0	8	0
	3-5	2	28	2
	6-10	3	33	3
	11-20	5	35	2
	21-50	2	24	1
	51-100	0	2	0
	>100	0	0	0
Jamestown	<3	2	0	0
	3-5	5	1	0
	6-10	12	10	1
	11-20	20	20	5
	21-50	12	16	15
	51-100	5	6	14
	>100	0	0	6
N. Carolina	<3	13	0	0
	3-5	27	0	0
	6-10	29	0	0
	11-20	38	0	0
	21-50	32	0	0
	51-100	5	0	0
	>100	1	0	0

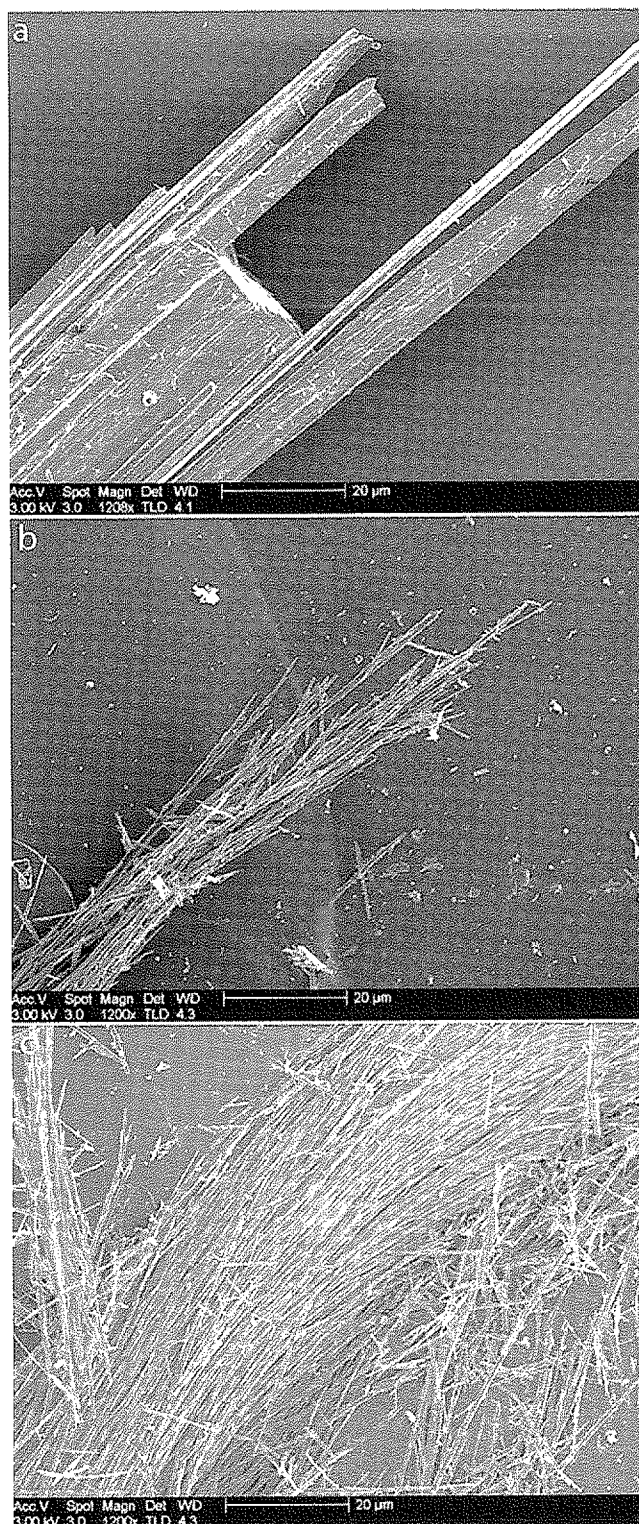


Figure 6: SEM images of the (a) NIST SRM 1867a tremolite, (b) Jamestown, California, and (c) North Carolina tremolites glued onto a glass slide. The magnification is the same for each photomicrograph and the degree of fibrosity increases as you move from (a) through (c).

light microscopy) and fibers and fiber bundles preferentially lie on a surface other than the (100).

The width requirement of asbestiform fibers is problematic in this study by PLM due to the limitations of resolving power. The measurement of extinction angles limits a particle to a width of around 1 to 2 μm , and the measurement of particle widths become highly subjective when particles are small. The extinction characteristics can be used as a first indicator of the fibrosity of the amphibole in question. If fibers from a bundle continue to display parallel extinction at smaller and smaller scales, this is an indication that the fibers are smaller fiber bundles not single crystals. Conversely, if fibers show oblique extinction, they are single crystals resting on the (010) face or (110) face or cleavage plane. Furthermore, if the circumstances are appropriate, both PLM and SEM may be necessary to fully characterize the fibril widths in order to determine accurately the true asbestiform amphibole content in mixed mineral environments or environmental exposure assessments. In a subsequent publication, an analytical method based on existing procedures incorporating these findings will be proposed for use in examining raw materials.

REFERENCES

1. Wylie, A.G. (1979) Optical properties of the fibrous amphiboles. *Annals of the New York Academy of Sciences*, 330, 600-605.
2. Stanton, M.F., Layard, M., Tegeris, A., Miller, E., May, M., Morgan, E., and Smith, A. (1981) Relation of Particle Dimension to Carcinogenicity in Amphibole Asbestos and Other Fibrous Minerals. *J. Natl. Cancer Inst.* 67, 965-975.
3. Pott, F. (1993) Fibre carcinogenicity in laboratory animals. *Fibre Toxicology* Ed. Warheit, D.B. Academic press Inc. 395-424.
4. Perkins, R.L. and Harvey, B.W. (1993) Method for the determination of asbestos in bulk building materials. U.S. Environmental Protection Agency EPA/600/R-93/116, Office of Research and Development, Washington, D.C.
5. CARB 435 (1991) Determination of Asbestos Content of Serpentine Aggregate. California Environmental Protection Agency. Air Resources Board.
6. Burdett, G. (1998) Quantitative measurement of asbestos and other fibres in bulk materials. Environmental Measurement Group, R42:70, IR/L/MF/98/02.
7. HSE (2005) Asbestos: The analysts guide for sampling, analysis and clearance procedure. HSE 248. UK Health and Safety Executive. ISBN 0-7176-2875-2. Her Majesty's Stationary Office.
8. Klinger, P.A., Nicholson, K.R., Hearl, F.J., and Jankovic, J.T. (1994). "Asbestos (bulk) by PLM." NIOSH Manual of Analytical Methods, Issue 2, Method Number 9002.
9. Verkouteren, J and Wylie, A.G. (2002) Anomalous optical properties of fibrous tremolite, actinolite, and ferro-actinolite. *American Mineralogist*, 87, 1090-1095.
10. Crane D.T. (1992). "Polarized Light Microscopy of Asbestos," OSHA Analytical Methods Manual, Method ID-191
11. Code of Federal Regulations (2006). "Interim Method of the Determination of Asbestos in Bulk Insulation Samples," 40 CFR Part 763, Appendix E to Subpart E.
12. Harris, K. E., Bunker, K.L., Strohmeier, B.R., Hoch, R., and Lee, R.J. (2007) "Discovering the True Morphology of Amphibole Minerals: Complementary TEM and FESEM Characterization of Particles in Mixed Mineral Dust," *Modern Research and Educational Topics in Microscopy*, A. Méndez-Vilas and J. Díaz, Eds., Formatex Microscopy Book Series, No. 3, Formatex Research Center, Badajoz, Spain, 2007.
13. Luce, D., Bugel, I., Goldberg, P., Goldberg, M., Salomon, D., Billon-Galland, M.A., Nicolau, J., Quenel, P., Fevotte, J., and Brochard, P. (2000) Environmental exposure to tremolite and respiratory cancer in New Caledonia: A case-control study. *American Journal of Epidemiology*, 151, 359-365.
14. Meeker, G.P., Lowers, H.A., Swayze, G.A., Van Gosen, B.S., Sutley, S.J., and Brownfield, I.K. (2006) Mineralogy and Morphology of Amphiboles Observed in Soils and Rocks in El Dorado Hills, California. USGS Open-File Report 2006-1362.
15. Gianfagna, A., Ballirano, P., Bellatreccia, F., Bruni, B., Paoletti, L., and Oberti, R., (2003) Characterization of amphibole fibres linked to mesothelioma in the area of Biancavilla, Eastern Sicily, Italy: *Mineralogical Magazine*, 67, 1221-1229.
16. Wylie, A.G. (1990), Discriminating Amphibole Cleavage Fragments from Asbestos: Rationale and Methodology, Proceedings of the VII International Pneumoconiosis Conference, Pittsburgh, p. 1065-1069 and Aerosols, p. 1065-1069, Proceedings of the Third International Aerosol Conference, Kyoto, Japan, September 24-27, 1990, Pergamon Press, New York, NY.
17. U.S. Environmental Protection Agency (2005) Response of the November 2005 National Stone, Sand, and Gravel Association report, Prepared by the R.J. Lee Group, Inc. "Evaluation of EPA's Analytical Data

From The El Dorado Hills Asbestos Evaluation Project"; EPA Region IX April 20, 2006, p9-10.

18. RJ Lee Group, Inc., (2005) Evaluation of EPA's Analytical Data from the El Dorado Hills Asbestos Evaluation Project, RJ Lee Group, Inc., Monroeville, Pennsylvania.

19. Davis J.M.G., Addison, J., McIntosh, C., Miller, B.R., and Niven K. (1991) Variations in the Carcinogenicity of Tremolite Dust Samples of Differing Morphology. *Annals of the New York Academy of Sciences*, 643, 473-490.

20. Brown, B.M. and Gunter, M.E. (2003) Morphological and Optical Characterization of Amphiboles from Libby, Montana U.S.A. by Spindle Stage Assisted – Polarized Light Microscopy. *The Microscope*, 51:3, 121-140.

21. Bloss, F.D. (1981) *The Spindle Stage: Principles and Practice*. Cambridge University Press, Cambridge, U.K.

22. Bandli, B.R. and Gunter, M.E. (2002) Identification and characterization of mineral and asbestos particles using the spindle stage and the scanning electron microscope: the Libby, Montana, U.S.A. amphibole asbestos as an example. *Microscope* 49, 191-199.

23. Verkouteren, J. and Wylie, A.G. (2000) The tremolite-actinolite-ferro-actinolite series: Systematic relationships among cell parameters, composition, optical properties, and habit, and evidence of discontinuities. *American Mineralogist*, 85, 1239-1254.

24. NIST (2003) Certificate of Analysis. Standard Reference Material 1867a, Uncommon Commercial Asbestos.

25. Su, S.C. and Bloss, F.D. (1984) Extinction angles for monoclinic amphiboles or pyroxenes: a cautionary note. *American Mineralogist*, 69, 399-403.